

# Robust formation of morphogen gradients

T. Bollenbach,<sup>1</sup> K. Kruse,<sup>1</sup> P. Pantazis,<sup>2</sup> M. Gonzalez-Gaitan,<sup>2</sup> and F. Jülicher<sup>1</sup>

<sup>1</sup>Max-Planck-Institute for Physics of Complex Systems,

Nothnitzer Str. 38, 01187 Dresden, Germany

<sup>2</sup>Max-Planck-Institute for Molecular Cell Biology and Genetics,

Pfotenhauer Str. 108, 01307 Dresden, Germany

(Dated: January 29, 2022)

## Abstract

We discuss the formation of graded morphogen profiles in a cell layer by nonlinear transport phenomena, important for patterning developing organisms. We focus on a process termed transcytosis, where morphogen transport results from binding of ligands to receptors on the cell surface, incorporation into the cell and subsequent externalization. Starting from a microscopic model, we derive effective transport equations. We show that, in contrast to morphogen transport by extracellular diffusion, transcytosis leads to robust ligand profiles which are insensitive to the rate of ligand production.

An essential feature during the development of an organism is the emergence of different cell types. This process, called cell differentiation, is intimately linked to the position of the cells in the organism. About fifty years ago, Turing suggested the existence of molecules that provide positional information for differentiating cells [1]. Turing proposed that these morphogens self-organize into patterns which structure the future organism. Pattern formation based on reaction-diffusion systems has been studied extensively [2, 3, 4]. Today, a number of proteins have been identified to act as morphogens. In contrast to Turing's original suggestion, morphogens are secreted from a spatially localized source and form a stable, long-ranged concentration gradient in the adjacent tissue [5]. There, cells detect the morphogen by receptors located on the cell surface and respond with patterns of gene expression that depend on the morphogen concentration. In this way, cell fate depends on the distance from the morphogen source and the interplay of several morphogen gradients originating from spatially distinct sources leads to the complex patterning of developing organisms. For this to be possible, the gene expression patterns must be formed with high precision and also need to be robust, i.e. they should not depend sensitively on parameters that are likely to fluctuate. Robust gene expression can result from the robustness of the morphogen concentration gradient [6, 7] or can be achieved by other mechanisms [8]. Interestingly, different species use very similar morphogens and a given species can use the same morphogen at different stages during development. An example are morphogens of the TGF- $\beta$  superfamily which exist in a wide range of organisms ranging from the fruit fly *Drosophila* to humans.

The formation of morphogen gradients is still poorly understood. In particular, it is not clear, how morphogens are transported in the tissue adjacent to the source. Several possibilities have been proposed. Secreted morphogen molecules might simply diffuse in the extracellular space between cells [9] and for some morphogens this indeed seems to be the dominant form of transport [10]. However, there is growing experimental evidence against simple diffusion for several morphogens [11, 12]. Other transport mechanisms, that have been proposed, include the bucket brigade, where molecules are "handed over" from one cell to adjacent cells [13], or transport by cell displacements in the tissue [14].

Another possibility is suggested by recent experiments on the morphogen Dpp [11]. Dpp belongs to the TGF- $\beta$  superfamily and patterns the developing wing discs of *Drosophila*. The wing disc is a sheet formed from one layer of cells that is the precursor of a wing. Fluor-

recently labeled Dpp was tracked in wing discs where it is secreted by a narrow strip of cells from where it spreads into the adjacent tissue. If all cells adjacent to the secreting cells are defective in the internalization of the morphogen into the cell, Dpp gradients extend only about two cells from the source as compared to 30 cells in a non-mutant fly. If only cells in a small patch close to the source show this defect, a pronounced transient depletion of the morphogen is observed behind the mutant patch during gradient formation. This suggests that Dpp is not simply diffusing through the extracellular space. It has been suggested that these observations can be described by a scenario where Dpp diffuses in the extracellular space, binds to and is released from receptors [15]. However, an analysis which takes into account more recent experimental results indicates that free diffusion alone cannot account for the observations [16]. An alternative suggestion is that long range transport of Dpp is generated by transcytosis, i.e. by repeated rounds of morphogen binding to cell surface receptors, internalization into the cell and subsequent externalization and release of the ligand from the receptor at a different point on the cell surface [17]. A simple model to describe transcytosis is illustrated in Fig. 1. Ligands spread from a stripe of secreting cells into a two-dimensional tissue. However, in many situations a one-dimensional description of ligand profiles as a function of the distance  $x$  to the source is appropriate [15, 16]. Transcytosis, can be characterized by rates  $k_{on}$  and  $k_{off}$  for receptor binding and unbinding of free ligands, as well as  $b_{int}$  and  $b_{ext}$  for internalization and externalization of ligand-bound receptors. Internalized morphogens are degraded with rate  $b_{deg}$ . The free diffusion of ligands in the narrow space between cells is characterized by the diffusion coefficient  $D_0$ . Diffusion alone does not lead to efficient long-range transport if the diffusion length  $\lambda_d = (D_0/e_{deg})^{1/2}$  is smaller than one or several cell diameters. Here,  $e_{deg}$  is the extracellular degradation rate.

On scales large compared to the cell diameter  $a$ , this model together with the assumption that receptors are also synthesized and degraded in the cells, leads to effective transport equations for the number densities  $\rho(t; x)$  of morphogens and  $\rho(t; x)$  of receptors given by

$$\partial_t \rho = \partial_x (D(\rho, r) \partial_x \rho - D(\rho, r) \partial_x r) - k(\rho, r) \rho \quad (1)$$

$$\partial_t r = \gamma_{syn}(\rho, r) - \gamma_{deg}(\rho, r) \quad (2)$$

Here,  $D(\rho, r)$  is an effective diffusion coefficient and  $k(\rho, r)$  an effective degradation rate that depend on both the ligand and receptor concentrations. Furthermore, a term exists which describes ligand currents induced by gradients of the receptor concentration. We

assume for simplicity that cells are non-polar such that externalization occurs with equal probability at any place on the cell surface. As a consequence, the resulting transport is non-directional. The kinetics of the receptor density is characterized by effective source and sink terms  $s_{\text{syn}}(\cdot)$  and  $s_{\text{deg}}(\cdot)$ . The dependences of the effective diffusion coefficient  $D$ , the degradation rate  $k$ , the coefficients  $D_{\text{syn}}$  and  $D_{\text{deg}}$  on the ligand and receptor concentrations can be calculated explicitly [18]. In order to keep our discussion simple, we focus here on the case where the surface receptor number per cell  $R$  is maintained constant. Then, ligand transport is described by a single nonlinear diffusion equation

$$\partial_t c = \partial_x (D(c) \partial_x c) - k(c) c \quad : \quad (3)$$

Explicit expressions of  $D(c)$  and  $k(c)$  are given in [22]. The coefficients are displayed as functions of the ligand concentration in Fig. 2. For small  $c$ ,  $D(c)$  and  $k(c)$  approach finite values, and the transport equation becomes linear. For large  $c$ ,  $D(c) = D_0 + c_1 c^{-2}$  with  $c_1 = a b_{\text{int}} k_{\text{off}} r = (4 k_{\text{on}})$ , where  $r = R/a$ . The effective diffusion coefficient  $D(c)$  decreases for large ligand concentration because receptors are increasingly occupied and not available for transport. A maximum of  $D$  occurs for intermediate values of  $c$ , if the ligand binding rate  $k_{\text{on}}$  exceeds a critical value. This implies that for small  $c$ ,  $D$  increases for increasing  $c$ . Similarly, the effective degradation rate exhibits for large  $c$  the asymptotic behavior  $k(c) = k_{\text{deg}} + c_2 c^{-1}$  where  $c_2 = b_{\text{deg}} b_{\text{int}} r = b_{\text{ext}}$ .

We solve Eq. (3) for  $x > 0$ , representing the space adjacent to the ligand source, and with boundary conditions  $j(x=0) = j_0$  and  $j=0$  for large  $x$ . Here,  $j_0$  is proportional to the rate of ligand secretion in the source. In this situation, a graded ligand profile is generated and maintained in the steady state, see Fig. 3.

The effect of the source is captured by the boundary condition on the current  $j = j_0$  at  $x=0$ , where  $j = -D(c) \partial_x c$ , see Eq. (3). If initially at time  $t=0$  ligand is absent  $c=0$ , the ligand spreads for  $t>0$  into the region  $x>0$ , and builds up a gradient. In the steady state, the total ligand concentration decreases monotonically with increasing distance from the source. The steady state satisfies  $\partial_x j + k(c) c = 0$  and is reached on a time scale of the order of  $1/k(c=0)$ . The corresponding ligand distribution  $c(x)$  obeys

$$x = \int_{(0)}^{Z(x)} d^0 D(c^0) = j(c^0) \quad ; \quad (4)$$

where the ligand current  $j$  in the steady state is given by

$$j(x) = \frac{2D_0}{\lambda} \left( \frac{c_1}{c_2} \right)^{\frac{1}{2}} \left( \frac{D_0}{k_0} \right)^{\frac{1}{2}} \left( \frac{x}{\lambda} \right)^{\frac{1}{2}} : \quad (5)$$

For small  $x$ , the ligand profile decays as  $\exp(-x/\lambda)$  with  $\lambda = (D_0/k_0)^{1/2}$ . In the case  $D_0 = 0$ , the steady state profile has a singularity at  $x = x^*$ :

$$(x - x^*)^{-1} \left( \ln(x - x^*) \right)^{-1/2} \quad (6)$$

Choosing  $j_0 > 0$  ensures  $x^* < 0$  such that  $x^*$  is not physically accessible. This singularity results from the asymptotic behavior of the current  $j$  for large  $x$ :  $j(x) \sim j_0^2 + 2e_{deg}c_1 \ln(x/\lambda) + 2c_1c_2(1/\lambda - 1/\lambda_0)$ . Here,  $\lambda_0$  denotes a characteristic ligand concentration beyond which the limit of large ligand concentration holds. Therefore the current diverges as  $j^2 \sim 2e_{deg} \ln(x/\lambda)$ . Note, that for  $e_{deg} = 0$  the current reaches for large  $x$  a finite maximal value  $j_{max}$  and the corresponding steady state ligand profile diverges as  $c_1 = [j_{max}(x - x^*)]$ .

The singular behavior of the steady state profile near  $x = x^*$  has remarkable consequences for the robustness of gradient formation. Such a robustness can be quantified by an appropriate response function of the system [6]. We define the robustness  $R(j_0) := a(j_0 \partial_{j_0} x(x))^{-1}$ , where the function  $x(x)$  is given by Eq. (4). It becomes large if changes of  $j_0$  have little influence on the ligand profile in the steady state. Here, a robustness of  $R = 1$  implies that under a 100% increase of  $j_0$  the position at which the ligand profile attains any fixed value is displaced by about one cell diameter  $a$ . Thus for  $R \gg 1$ , cells in the target tissue cannot detect variations of the ligand concentration due to significant changes of  $j_0$ , while for  $R \ll 1$  the steady state profile is strongly affected, see Fig. 3. Note, that  $R$  is independent of  $\lambda$ . Indeed,  $R$  can be rewritten as

$$R = a(j_0 \partial_{j_0} x)^{-1} = a \partial_{j_0} j_0 = D_0/k_0 = j_0 \quad (7)$$

where  $j_0 = j(x=0)$  and Eqs. (4) and (5) have been used. The robustness is thus completely determined by the ratio of the effective degradation rate and the ligand current at  $x = 0$ . High degradation rates and small currents lead to a robust gradient. Using the asymptotic behavior of the steady state profile for  $D_0 = 0$ , we find that the robustness increases rapidly for large currents  $j_0$  as  $R \sim j_0^{-1} e^{j_0^2/\lambda_c^2}$  with  $\lambda_c^2 = 1/2c_1e_{deg}$ . For small  $j_0$ ,  $R$  approaches a constant.

The situation is different if  $D_0$  is finite. In this case, both  $k(\cdot)$  and  $D(\cdot)$  are nonvanishing and constant for large  $x$  and consequently Eq. (3) becomes linear in this limit. The steady state profile for  $c_1=D_0$  behaves as  $\exp(-x/a)$ . In the interval  $\tau < c_1=D_0$  the ligand profile is well described by Eq. (6), while for small  $\tau$ ,  $\exp(-x/a)$ . As a consequence of finite  $D_0$ , the robustness approaches a finite value  $R_{\max} = a/a_d$  for large  $j_0$ . For  $a_d < a$ , this implies  $R > 1$  for large  $j_0$  and cells in the target tissue are insensitive to variations of  $j_0$  by a factor of two. The robustness is displayed in Fig. 4 as a function of  $j_0$  for different values of  $a_d=a$ .

Finally, we briefly discuss how the transport Eq. (3) is derived from a microscopic model. We denote the number of free ligands in the space between cell  $n$  and  $n+1$  by  $L_n$  and the numbers of receptor-bound ligands inside cell  $n$  by  $S_n^{(i)}$ . Similarly, we introduce the numbers  $S_n^{(r)}$  and  $S_n^{(l)}$  of receptor-bound ligand on the right and left surface of cell  $n$ , respectively, see Fig. 1. The dynamics of these quantities is given by

$$\partial_t L_n = k_o (S_n^{(r)} + S_{n+1}^{(l)}) - k_{on} (R - S_n^{(r)} - S_{n+1}^{(l)}) L_n - \partial_{\text{deg}} L_n \quad (8)$$

$$\partial_t S_n^{(r)} = k_o S_n^{(r)} + k_{on} \frac{R}{2} S_n^{(r)} L_n - b_{\text{int}} S_n^{(r)} + \frac{1}{2} b_{\text{ext}} S_n^{(i)} \quad (9)$$

$$\partial_t S_n^{(l)} = k_o S_n^{(l)} + k_{on} \frac{R}{2} S_n^{(l)} L_{n-1} - b_{\text{int}} S_n^{(l)} + \frac{1}{2} b_{\text{ext}} S_n^{(i)} \quad (10)$$

$$\partial_t S_n^{(i)} = b_{\text{ext}} S_n^{(i)} + b_{\text{int}} (S_n^{(l)} + S_n^{(r)}) - b_{\text{deg}} S_n^{(i)} \quad (11)$$

On large scales, we describe the ligand profiles by the densities  $l(x) = L_n/a$ ,  $s(x) = S_n^{(i)}/a$  and  $s_{\pm}(x) = [S_n^{(l)} - S_n^{(r)}]/a$ , where  $x = na$ . Because transport on large scales  $L$  is governed by time scales  $\tau_L \propto L^2/D$  which are long compared to the relaxation time on the cellular scale  $\tau_a \propto a^2/D$ , three of the dynamic equations can be adiabatically eliminated. The effective Eq. (3) for the total ligand density  $\phi = l + s + s_{\pm}$  follows by taking a continuum limit [18]. A comparison of the full solutions of Eqs. (8)–(11) to Eq. (3) is shown in Fig. 3, demonstrating that the effective transport Eq. (3) captures the behavior of the microscopic model.

In conclusion, we have developed a general theoretical framework for ligand transport and the generation of characteristic ligand profiles via transcytosis. Cell differentiation is triggered at threshold levels of morphogen concentration. The robustness of patterning has been demonstrated experimentally under conditions where  $D_{pp}$  was overexpressed [11, 16, 19]. Reliable patterning can be achieved by robustly generating morphogen profiles. We have defined the robustness of steady state ligand profiles with respect to the rate of ligand secretion  $j_0$ . We find that transcytosis naturally leads to a large robustness of the profile.

Free extracellular diffusion reduces robustness significantly if the diffusion length  $\lambda_d$  exceeds several cell sizes. The origin of robustness in transcytosis are nonlinearities in the ligand current. A similar mechanism based on nonlinear degradation alone permits the robust formation of gradients in a free diffusion model [6]. Robustness can also be achieved by other nonlinear effects [7].

In the general case where both ligand and receptor densities are taken into account, new phenomena appear [18]. In particular ligand currents can be driven by receptor gradients. Furthermore, ligand gradients are accompanied by a gradient in the receptor density as is indeed observed experimentally [11, 20]. In addition, if cells possess a polarity and define a direction in the tissue, transcytosis can lead to directed transport. Finally, it is straightforward to generalize the concepts presented here to higher dimensions.

The effects discussed here become important if the diffusion length  $\lambda_d$  is smaller than the range  $\lambda \sim 30a$  of the gradient. From experiments where endocytosis has been blocked in the target tissue, we estimate  $\lambda_d \sim 2a$  [1]. The rates of transcytosis have to be sufficiently large to guarantee gradient formation within the experimentally observed times of about  $k(0)^{-1} \sim 8$  hours. Assuming that the rates  $k_{on}R$ ,  $k_o$ ,  $b_{int}$ , and  $b_{ext}$  are of the order of  $1 \text{ min}^{-1}$ , we estimate  $D \sim a^2 \text{ min}^{-1}$ . This diffusion coefficient is sufficient to generate a gradient over a length  $\sim 30a$  during 8 hours. Numerical solutions to the transcytosis model (see Fig. 3) confirm this estimate. A rate of one per minute is larger than values measured in different but related systems [21] but is plausible for intracellular trafficking.

The values of the rate constants are difficult to measure while the effective diffusion coefficient and the effective degradation rates are more easily accessible in fluorescence recovery experiments. Our work suggests that if transcytosis dominates transport, morphogen gradients are robust with respect to morphogen overexpression. This can be directly tested in future experiments.

---

[1] A. M. Turing, Philosophical Transactions of the Royal Society of London Series B 237, 37 (1952).

[2] M. C. Cross and P. C. Hohenberg, Reviews of Modern Physics 65, 851 (1993), part 2.

[3] A. J. Koch and H. Meinhardt, Reviews of Modern Physics 66, 1481 (1994).

- [4] A. Gierer and H. Meinhardt, *Kybernetik* 12, 30 (1972).
- [5] L. Wolpert, *Journal of Theoretical Biology* 25, 1 (1969).
- [6] A. Eldar, D. Rosin, B. Z. Shilo, and N. Barkai, *Developmental Cell* 5, 635 (2003).
- [7] A. Eldar, R. Dorfman, D. Weiss, H. Ashe, B. Z. Shilo, and N. Barkai, *Nature* 419, 304 (2002).
- [8] B. Houchmandzadeh, E. Wieschaus, and S. Leibler, *Nature* 415, 798 (2002).
- [9] F. Crick, *Nature* 225, 420 (1970).
- [10] N. McDowell, A. M. Zom, D. J. Crease, and J. B. Gurdon, *Current Biology* 7, 671 (1997).
- [11] E. V. Entchev, A. Schwabedissen, and M. Gonzalez-Gaitan, *Cell* 103, 981 (2000).
- [12] T. Y. Belenkaya et al., *Cell* 119, 231 (2004).
- [13] M. Kerszberg and L. Wolpert, *Journal of Theoretical Biology* 191, 103 (1998).
- [14] S. Pfeifer, C. Alexandre, M. Calleja, and J. P. Vincent, *Current Biology* 10, 321 (2000).
- [15] A. D. Lander, Q. Nie, and F. Y. M. Wan, *Developmental Cell* 2, 785 (2002).
- [16] K. Kruse, P. Pantazis, T. Bollenbach, F. Julicher, and M. Gonzalez-Gaitan, *Development* 131, 4843 (2004).
- [17] E. V. Entchev and M. A. Gonzalez-Gaitan, *Trac* 3, 98 (2002).
- [18] T. Bollenbach et al., to be published.
- [19] S. Morimura, L. Maves, Y. Chen, and F. M. Hermann, *Developmental Biology* 177, 136 (1996).
- [20] A. A. Teleman and S. M. Cohen, *Cell* 103, 971 (2000).
- [21] D. A. Lauburger and J. J. Lindemann, *Receptors: models for binding, trafficking, and signalling* (Oxford University Press, 1993).
- [22] We find  $k(\cdot) = C + (\cdot) [b_{deg} b_{int} = 2b_{ext} (b_{ext} + b_{int})] + e_{deg} k_o = C(\cdot)] =$ . For  $D_0 = 0$ , we furthermore have  $D(\cdot) = [a^2 b_{ext} b_{int} k_o - r C(\cdot)] = [4A(\cdot) [2rk_o (b_{ext} + b_{int}) + b_{int} C(\cdot)]]$ . In these expressions  $= ak_{on}$ ,  $A(\cdot) = 4b_{ext} (b_{ext} + b_{int})^2 r + (b_{int} r + b_{ext} B_+(\cdot))^2$ ,  $B_+(\cdot) = k_o + (\cdot - r)$ ,  $C(\cdot) = b_{int} r - A(\cdot) - b_{ext} B_+$ .



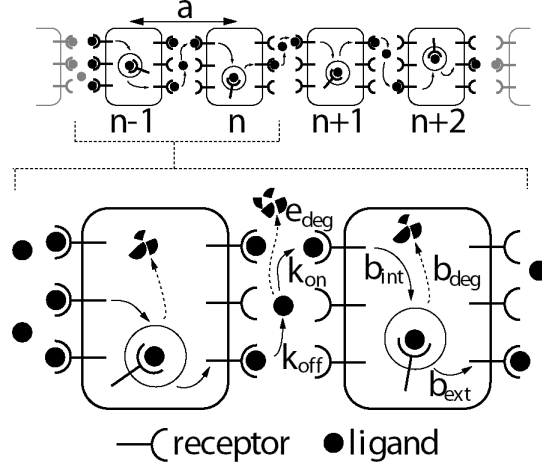


FIG . 1: Schematic representation of transport by transcytosis in a chain of cells of diameter  $a$  indexed by  $n$ . The rates of ligand-receptor binding and unbinding, internalization and externalization of ligand-receptor pairs are denoted  $k_{on}$ ,  $k_{off}$ ,  $b_{int}$  and  $b_{ext}$ . Degradation of ligand occurs inside the cells with rate  $b_{deg}$  and in the extracellular space with rate  $e_{deg}$ .

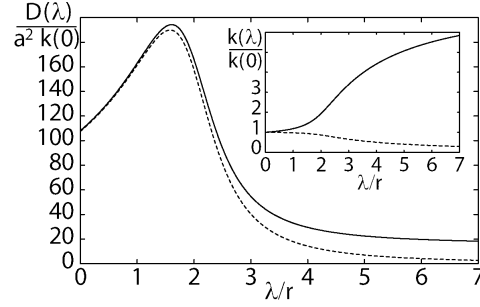


FIG . 2: Effective diffusion coefficient  $D(\lambda)$  as a function of ligand concentration  $\lambda/r$  for  $D_0 = a^2 b_{deg} = 10$  (solid line) and  $D_0 = 0$  (dashed line). Inset: effective degradation rate  $k(\lambda)$  as a function of  $\lambda/r$  for  $e_{deg} = 0$  (dashed line) and  $e_{deg} = b_{deg} = 5$  (solid line). Parameters are:  $b_{int} = b_{deg} = b_{ext} = 3 \cdot 10^3$ ,  $k_{on} R = b_{deg} = 1 : 1 \cdot 10^4$ ,  $k_{off} = b_{deg} = 7 \cdot 10^2$ .

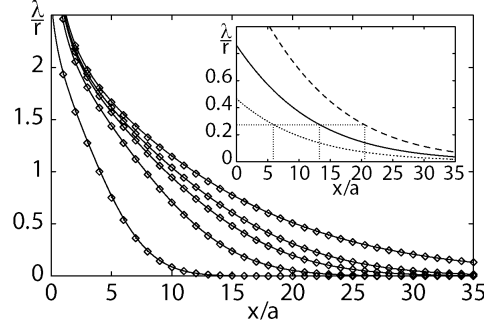


FIG. 3: Ligand densities  $\lambda(x)$  in the presence of a source at  $x = 0$  at different times  $b_{\text{deg}}t = 0.18; 0.54; 0.9; 1.26$  during gradient formation and in the steady state. Lines indicate solutions to Eq. (3), while symbols indicate solutions to Eqns. (8)–(11) for comparison. The robustness of the steady state profile is  $R = 470$ . Parameters as in Fig. 2 with  $D_0 = 0$ ,  $j_0 = b_{\text{deg}}R = 70$  and  $j = 0$  at  $x = a = 50$ . Inset: steady state ligand profiles for same parameters but  $j_0 = b_{\text{deg}}R = 7$  where  $R = 0.1$ . The profile (solid line) is strongly affected by halving (dotted line) or doubling (dashed line) the ligand current of the reference state.

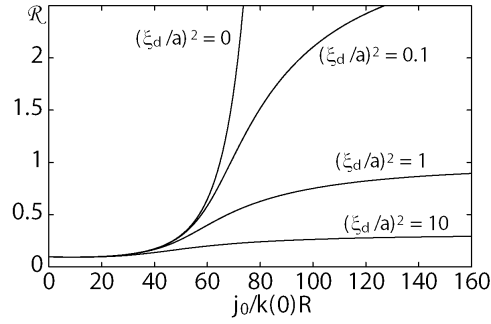


FIG. 4: Robustness  $R$  of steady state ligand profiles as a function of the ligand current  $j_0$  from the source for different values of the ratio of the diffusion length  $\xi_d$  and the cell size  $a$ . Parameters as in Fig. 2.